

Development of a Flat Membrane Microchannel Packed-  
Bed Reactor for Scalable Aerobic Oxidation of Benzyl  
Alcohol in Flow

*Gaowei Wu,<sup>[a]</sup> Enhong Cao,<sup>[a]</sup> Peter Ellis,<sup>[b]</sup> Achilleas Constantinou,<sup>† [a]</sup> Simon  
Kuhn,<sup>[c]</sup> Asterios Gavriilidis<sup>\* [a]</sup>*

[a] Department of Chemical Engineering, University College London, Torrington Place,  
London, WC1E 7JE, U.K.

[b] Johnson Matthey Technology Centre, Blounts Court, Sonning Common, Reading RG4  
9NH, U.K.

[c] Department of Chemical Engineering, KU Leuven, Celestijnenlaan 200F, 3001 Leuven,  
Belgium

Corresponding author: \*E-mail: [a.gavriilidis@ucl.ac.uk](mailto:a.gavriilidis@ucl.ac.uk).

†Current address: Division of Chemical and Petroleum Engineering, School of Engineering, London South  
Bank University, 103, Borough Road, London SE1 0AA, U.K.

## ABSTRACT

A Teflon AF-2400 flat membrane microchannel reactor was designed and demonstrated for safe and scalable oxidation of solvent-free benzyl alcohol with molecular oxygen on Au-Pd/TiO<sub>2</sub> catalyst. The microchannel reactor employed a mesh-supported Teflon AF-2400 flat membrane, with gas and liquid channels on each side. Catalyst particles were packed in the liquid flow channel. Operation with 20 bara pressure difference between the gas and the liquid phases was possible at 120 °C. Pervaporation of organics through the membrane was experimentally measured to assure that the organic vapour concentration remains below the lower explosive limit during the reaction. The effect of oxygen pressure was studied, and the oxygen was shown to have a positive effect on the oxidation of benzyl alcohol. A conversion of benzyl alcohol of 70% with 71% selectivity to benzaldehyde was obtained at 1150 g<sub>cat</sub>·S/g<sub>alcohol</sub>, 8.4 bara oxygen pressure and 10 bara liquid pressure. Doubling the membrane thickness led to a 20% drop of oxygen consumption rate, indicating the main oxygen transfer resistance not existing in the membrane. When changing the catalyst particle size and the liquid flow rate, no significant effect was observed on the oxidation reaction rate. An effectiveness factor approach is proposed to predict the effect of oxygen permeation and transverse mass transfer on the catalyst packed in the membrane reactor, which suggests that the oxidation of benzyl alcohol on the highly active Au-Pd/TiO<sub>2</sub> catalyst is controlled by the oxygen transverse mass transfer in the bulk liquid within the catalyst bed. Scale-up of the flat membrane microchannel reactor was demonstrated through widening the liquid channel width by ~10 times, which increased the reactor productivity by a factor of 8.

**Keywords:** Gold-palladium catalyst; Teflon AF-2400 membrane; membrane microchannel reactor; aerobic oxidation of alcohol; effectiveness factor.

## 1. Introduction

Oxidation of alcohols is one of the most important processes in organic chemistry and often performed with stoichiometric inorganic reagents [1-3]. To improve the atom efficiency and reduce the environmental costs, heterogeneous catalysts have been developed, and significant advances have been reported [4-8]. However, large-scale applications of aerobic oxidation of alcohols are still limited by potential safety issues caused by the oxidant-organic reactant mixtures [5, 9, 10].

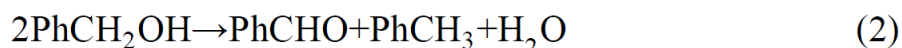
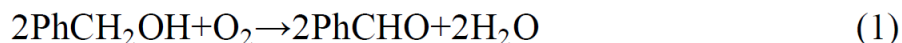
Recently, several approaches have been proposed to ensure intrinsic process safety. Stahl and co-workers [11, 12] reported a continuous-flow tube reactor for homogeneous Pd-/Cu-catalyzed

aerobic oxidation of primary alcohols to aldehydes, where a dilute oxygen source (8-9% oxygen in nitrogen) was used to avoid the oxygen/organic mixture entering the explosive regime. Zotova et al. [13] developed a safe process for aerobic oxidation of alcohols with a commercially available XCube™ reactor, by pre-mixing and saturating the liquid with the gaseous reactant (oxygen or air) before reaching the catalyst bed.

Among these approaches, membrane reactors have attracted attention, since a membrane can act as a well-defined contacting interface for gas and liquid phases [14-16]. The membrane allows strict control of the reactants and avoids direct mixing of oxygen with organic reactants. A ceramic membrane reactor was developed in our group for oxidation of benzyl alcohol with pure oxygen [17]. The reactor consisted of a commercially-available tubular ceramic membrane with catalyst packed in the inner tube. The liquid phase flowed through the inner tube, and pure oxygen flowed in the opposite side of the membrane. Deficiency of oxygen in the catalyst bed area was suggested to occur for relatively fast catalytic system. As one type of amorphous fluoroplastics, Teflon AF-2400 membrane has gained popularity, since it has high permeabilities to gases and excellent chemical compatibility [18]. The Ley group first developed a Teflon AF-2400 tube-in-tube membrane microreactor and applied it to various reactions such as key C-C, C-N, and C-O bond forming and hydrogenation reactions [19-21]. Chaudhuri et al. [22] used the tube-in-tube reactor to saturate the liquid stream with oxygen/air for heterogeneously catalytic oxidation of alcohols. An *in-situ* continuous supply of oxygen through the membrane to the catalyst was also realized through packing the solid catalyst inside the inner tube of the tube-in-tube reactor [23]. This contributed to a significant improvement in both conversion and selectivity. Greene et al. [24] developed a “tube-in-shell” membrane microreactor with inexpensive PTFE tubing for homogeneous and heterogeneous oxidation of alcohols with molecular oxygen. Though the price of common fluoropolymers such as PTFE membrane is much lower than that of Teflon AF-2400 membrane, the high oxygen permeability of Teflon AF-2400 membrane makes it attractive for oxidation of solvent-free benzyl alcohol within several-centimetre catalyst bed.

Some potential drawbacks still exist for the packed tube-in-tube membrane reactor. The gas phase present in the annulus between the inner and outer tubes could possibly act as a heat transfer resistance for exothermic reactions, due to its relatively low thermal conductivity. The scale-up of the tube-in-tube reactor is not facile, since increasing the membrane diameter will result to a proportional increase in radial mass transfer resistance under laminar flow [25]. In an attempt to address these issues, a Teflon AF-2400 flat membrane microchannel reactor is developed in this study. Oxidation of benzyl alcohol is performed on Au-Pd/TiO<sub>2</sub> catalyst, which has high activity and good reusability [26]. Oxidation of benzyl alcohol on Au-Pd/TiO<sub>2</sub> is considered to comprise of two main parallel reactions, the oxidation reaction (eq 1) and the disproportionation reaction (eq 2) [27, 28]. Both the oxidation and disproportionation of benzyl alcohol can form the target product,

benzaldehyde, while the toluene by-product is generated from disproportionation. In our recent kinetic study, hydrogenolysis of benzyl alcohol to toluene was found to play an important role for toluene formation, but at oxygen deficient conditions disproportionation prevails [29]. Hence, in our discussions in this work the hydrogenolysis pathways are neglected, since in the packed-bed membrane reactor (as will be shown) there is deficiency of oxygen supply. The amount of consumed oxygen during the reaction could be calculated based on the conversion of benzyl alcohol and selectivities to benzaldehyde and toluene [23].



## 2. Experimental Section

### 2.1 Catalyst preparation

A nominal 1 wt% bimetallic Au-Pd/TiO<sub>2</sub> catalyst was prepared by co-impregnation, similar to previous work [26, 30]. TiO<sub>2</sub> (Degussa, P25) was first suspended in demineralized water by stirring, and then HAuCl<sub>4</sub>·3H<sub>2</sub>O (Johnson Matthey) and PdCl<sub>2</sub> (Johnson Matthey) with Au-to-Pd weight ratio equivalent to 1:19 was added. The resultant slurry was spraydried (nozzle temperature 220 °C), and then calcined in static air at 400 °C for 1 h. The metal content was analysed by ICP-AES and found to be 0.05 wt% Au and 0.85 wt% Pd, while the metal particle size as observed by TEM was 1–2 nm. The powder was pelletized, crushed, and sieved to the desired particle size range.

### 2.2 Design of flat membrane microchannel reactor

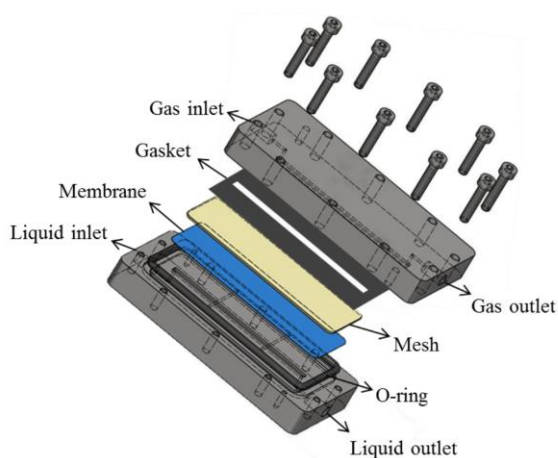


**Figure 1.** Schematic of the flat membrane microchannel reactor consisting of gas and liquid flow plates with viton gasket, stainless steel mesh, and Teflon AF-2400 membrane.

The flat membrane microchannel reactor designed in this work consisted of several layers, which are shown in Figure 1. From the bottom to the top, these are a liquid flow plate machined in 316 stainless steel (channel size length: 75 mm; width: 3 mm; depth: 1 mm), a Teflon AF-2400 membrane (length: 85 mm; width: 30 mm; thickness: 0.07 mm; Biogeneral), a 304 stainless steel mesh (length: 85 mm; width: 30 mm; thickness: 0.05 mm; hole size: 76  $\mu\text{m}$ ; open area: 23%; Industrial Netting; shown in Figure S1, Supporting Information), viton gasket (length: 85 mm; width: 30 mm; thickness: 1 mm; open area length: 75 mm; width: 3 mm; Altec) and a gas flow plate (with the same channel size and material to the liquid flow plate). The sealing of the reactor was achieved by compressing the membrane and the gasket with screws; the membrane also acted as a gasket for the liquid flow plate. An O-ring groove was machined in the liquid flow plate, which allowed also a sintered metal plate to be applied as the membrane support. Two holes were drilled in both liquid and gas channel plates (perpendicular, 1 mm away from the channel) for thermocouple insertion. A small circular piece of another nickel mesh (diameter:  $\sim 2$  mm; thickness: 0.05 mm; hole size: 25  $\mu\text{m}$ ; Tecan) was placed between the liquid outlet and the fitting for retaining the catalyst. After assembling the reactor, 50 mg silica beads (particle size: 90-15  $\mu\text{m}$ ) were packed into the liquid channel followed by the Au-Pd/TiO<sub>2</sub> catalyst particles, with the help of a vacuum pump. The length of the 100 mg catalyst bed was  $\sim 5$  cm.

The reactor was placed on a hotplate (Gallenkamp) fitted with a thermocouple. The thermocouple was inserted in the hole beneath the catalyst bed for temperature measurement and control. To decrease heat loss, an insulation cap (insulation thickness:  $\sim 2$  cm; WDS® Ultra, Morgan) was made to cover the reactor. The temperature differences between the gas and the liquid flow plates during the reaction at 120 °C was measured through the thermocouples in the other holes, which was less than 3 °C.

### 2.3 Scale-up of the flat membrane microchannel reactor

To scale up the flat-membrane microchannel reactor, the gas/liquid channel widths were increased to 32 mm. CFD modelling was performed with COMSOL Multiphysics® Modelling Software (using Navier-Stokes and the continuity equations) to ensure the flows distributed uniformly in the channels. The gas flow channels were 1 mm deep in the gas flow plate, and pillars and fins were designed to distribute the gas flow and assist in supporting the membrane. The length of the liquid flow channel was 68 mm, with a depth of 0.5 mm. Distribution channels were machined at the inlet and outlet of the liquid flow plate. Sintered metal filters (304 stainless steel; Mott, grade 0.1) were inserted between the liquid distribution channels and the liquid channel to retain the catalyst particles. To better seal the top edge of the catalyst filters, a Kalrez® gasket (thickness: 0.5 mm; DuPont™) was added between the liquid flow plate and the membrane, which also made the total depth of liquid channel (machined liquid channel plus open area of the Kalrez® gasket) close to 1 mm. The catalyst was packed in the liquid flow channel and an opening (diameter: 2 mm) was drilled on one side of the liquid flow plate for catalyst packing. The scaled-up reactor was heated with two silicone rubber heaters (Watlow, wire-wound elements 020050C2). The whole reactor was insulated by an insulation cap (insulation thickness:  $\sim 2$  cm; WDS® Ultra, Morgan) and the temperature difference within the reactor was  $\pm 2$  °C at set temperature of 120 °C.

## 2.4 Reaction experiments

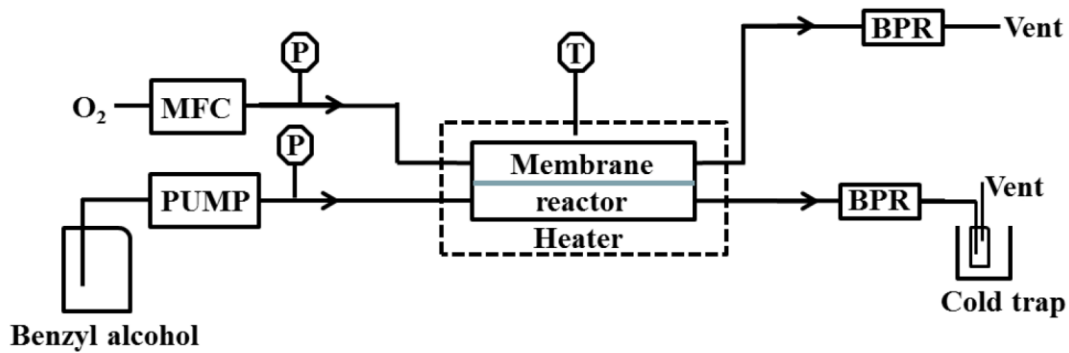


**Figure 2.** Schematic of the experimental set-up (MFC: mass flow controller; P: pressure sensor; T: thermocouple; BPR: back pressure regulator)

A schematic of the experimental set-up is shown in Figure 2. Neat benzyl alcohol (99.0%, Sigma-Aldrich) was delivered into the microchannel reactor with a HPLC pump (Knauer P2.1S). An adjustable back pressure regulator (BPR) (Zaiput, BPR-01) was used at the liquid outlet to maintain the liquid pressure. Pure oxygen was regulated by a mass flow controller (Brooks, GF40 series) and directed to the gas inlet of the reactor. A BPR (1-11 bara, Swagelok, K series) was connected at the gas outlet to maintain the gas pressure. The pressures of the gas and liquid phases were monitored by pressure sensors (Zaiput, Hastelloy/PFA wetted parts) placed upstream of the reactor.

The effluent from the liquid outlet was collected in a cold trap (ice-water bath) and quantitatively analysed by a gas chromatograph (Agilent 7820A) fitted with a DB-624 capillary column and a flame ionization detector. Benzyl alcohol conversion ( $X$ ) and selectivity ( $S_i$ ) of each product were calculated according to the following equations:

$$X = \frac{C_{BnOH,in} - C_{BnOH,out}}{C_{BnOH,in}} \times 100\% \quad (3)$$

$$S_i = \frac{C_i \cdot \nu_i}{C_{BnOH,in} \cdot X} \times 100\% \quad (4)$$

where  $C_{BnOH,in}$  and  $C_{BnOH,out}$  are the concentration of benzyl alcohol at the inlet and outlet, respectively and  $\nu_i$  is the number of moles of benzyl alcohol consumed for the production of 1 mole of product  $i$ . In this study,  $S_B$  and  $S_T$  stand for selectivities to benzaldehyde and toluene, respectively.

Catalyst contact time ( $CCT$ ) was used to characterise the reaction time of benzyl alcohol, and defined as:

$$CCT = \frac{m_{cat}}{v\rho} \quad (5)$$

where  $m_{cat}$  is the mass of catalyst,  $v$  is the inlet volumetric flow rate of benzyl alcohol,  $\rho$  is the density of benzyl alcohol at 20 °C. For each experiment, at least three samples were collected and the results were averaged. The errors for the conversion and selectivities were less than  $\pm 2\%$ . Oxygen consumption rates ( $OCR$ , at standard temperature and pressure, 0 °C and 1 bara, STP) were calculated by

$$OCR = \frac{1}{2} \cdot F_{BnOH,in} \cdot X \cdot (S_B - S_T) \cdot \tilde{V}_{O_2} \quad (6)$$

where  $F_{BnOH,in}$  is the molar flow rate of benzyl alcohol,  $\tilde{V}_{O_2}$  is the molar volume of oxygen at STP.

Average turnover frequency ( $TOF$ ) was calculated to better represent the reaction rate, where  $TOF_{total}$ ,  $TOF_O$  and  $TOF_D$  correspond to the overall reaction, the oxidation reaction and the disproportionation reaction, respectively.

$$TOF_{total} = \frac{F_{BnOH,in} \cdot X}{n_{metal}} \quad (7)$$

$$TOF_O = \frac{F_{BnOH,in} \cdot X \cdot (S_B - S_T)}{n_{metal}} \quad (8)$$

$$TOF_D = \frac{2F_{BnOH,in} \cdot X \cdot S_T}{n_{metal}} \quad (9)$$

where  $n_{metal}$  is the moles of the metals contained in the packed catalyst.

### 3. Results and Discussion

#### 3.1 Operation pressure and solvent pervaporation

Initially, the operating pressure range of the reactor was studied without any catalyst packed. Reactor temperature was kept at 120 °C and atmospheric pressure was applied in the gas phase. The pressure in the liquid phase was gradually increased to 21 bara (20 bara pressure difference) and kept for 0.5 h. No leaking was detected. Noticably, only slight change of the shape of the membrane was observed after testing at such pressure difference and temperature (shown in Figure S2a). In contrast, obvious membrane shape change was observed when no mesh was used to support the membrane (shown in Figure S2b). No membrane breakage was observed, since the membrane touched the bottom of the gas channel due to the shape change. It should be noted that in our previous tube-in-tube membrane microreactor, the Teflon AF-2400 inner tube (1 mm thickness) broke when  $\sim 12$  bara pressure difference was applied at 120 °C. This indicates the flat membrane

microchannel reactor could expand the operating pressure range of the Teflon AF-2400 membrane at elevated temperature.

Though direct mixing of oxygen with organic reactants is avoided by using the membrane reactor, organic vapour may appear in the gas phase through pervaporation. To assure that the organic vapour concentration remained outside the explosive limits, the pervaporation of the reactant and the main products (benzyl alcohol, benzaldehyde and toluene) through the membrane were experimentally measured and the details are shown in the Supporting Information. The pervaporation rate of toluene through the membrane was found to be the highest, which was 32.2 mg/h (this corresponds to 14.3 mg/h/cm<sup>2</sup> membrane area). It corresponds to 0.13 mL/min toluene vapour in the gas phase channel at STP. This highlights the necessity of using continuous flow in the gas phase to dilute the pervaporating organics. To keep the organic vapour concentration lower than 1 vol% (which is the lower explosive limit for toluene in air at 6 bara and 120 °C) [31], an oxygen flow rate of 15 mL/min at STP was utilized in the following experiments.

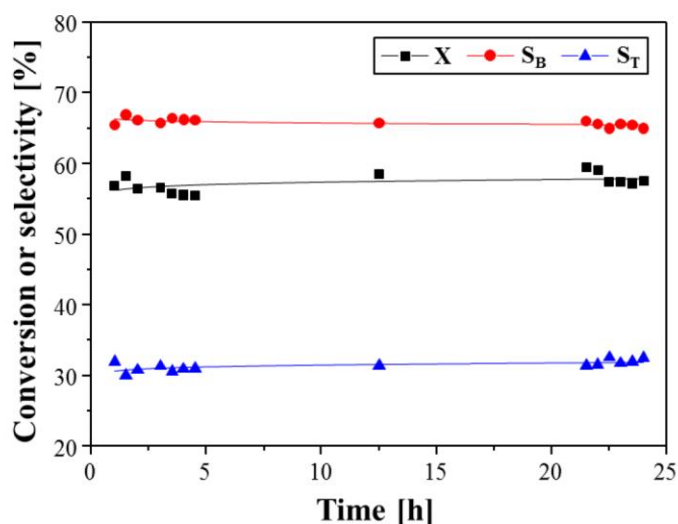


**Figure 3.** Stability study of the Au-Pd/TiO<sub>2</sub> catalyst in the flat membrane microchannel reactor. Conversion and selectivities are shown as a function of operation time. Reaction conditions: Au-Pd/TiO<sub>2</sub> catalyst (90-125 μm), 100 mg; neat benzyl alcohol, 10 μL/min; catalyst contact time, 577 g<sub>cat</sub>·s/g<sub>alcohol</sub>; oxygen pressure, 8.4 bara; liquid pressure, 10 bara; reaction temperature, 120 °C.

### 3.2 Catalyst stability

To evaluate the performance of the Au-Pd/TiO<sub>2</sub> catalyst and the reactor, a stability study was initially conducted and the results are shown in Figure 3. The catalyst contact time was 577 g<sub>cat</sub>·s/g<sub>alcohol</sub> and the conversion of benzyl alcohol was stable around 57% over 24 h. The selectivities to benzaldehyde and toluene, the two main products, also showed stable trends (66% and 31%, respectively). The selectivities to other minor products (dibenzyl ether, benzyl benzoate, *etc.*) were all less than 3% (not shown). These results demonstrate the high stability of the prepared Au-Pd/TiO<sub>2</sub> catalyst, as well as the excellent performance of the flat membrane microchannel reactor. The productivity of benzaldehyde was calculated to be 2.3 g<sub>B</sub>/(g<sub>cat</sub>·h).

### 3.3 Effect of oxygen pressure

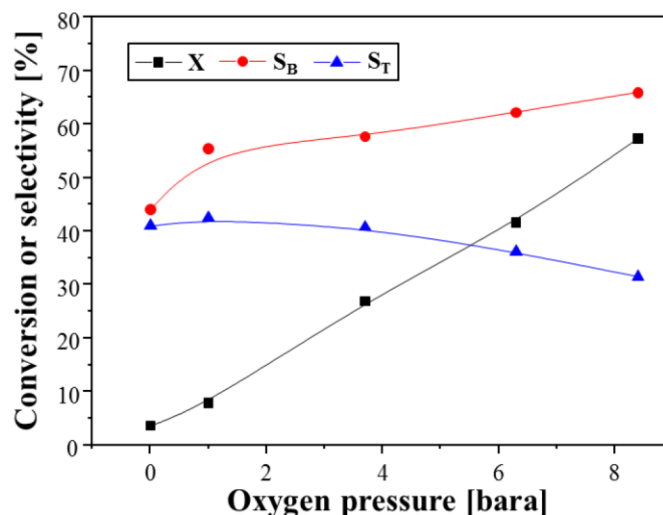


**Figure 4.** Effect of oxygen pressure on the conversion and selectivities during oxidation of benzyl alcohol in the flat membrane microchannel reactor. Reaction conditions: Au-Pd/TiO<sub>2</sub> catalyst (90-125 μm), 100 mg; neat benzyl alcohol, 10 μL/min; catalyst contact time, 577 g<sub>cat</sub>·s/g<sub>alcohol</sub>; liquid pressure, 10 bara; reaction temperature, 120 °C.

To explore the effect of oxygen pressure on the oxidation of benzyl alcohol in the flat membrane microchannel reactor, oxygen pressure was changed from 0 to 8.4 bara. Other reaction conditions were kept the same. From Figure 4, the conversion of benzyl alcohol was observed to be 4% at 0 bara oxygen pressure (nitrogen flowed through the gas channel at atmospheric pressure). Almost equimolar amounts of benzaldehyde (44%) and toluene (41%) were formed due to the disproportionation of benzyl alcohol [27, 28]. With oxygen pressure increasing, the conversion gradually rose and reached 57% at 8.4 bara. The selectivity to benzaldehyde also increased from 44% to 66% within the investigated oxygen pressure range. Correspondingly, the selectivity to toluene drop from 41% to 31%. The same behaviour was also observed in previous tube-in-tube membrane microreactor [23]. When increasing the oxygen pressure from 3 to 7 bara, the conversion of benzyl alcohol increased from 22% to 42% with the selectivity to benzaldehyde from 61% to 65% at catalyst contact time 115 g<sub>cat</sub>·s/g<sub>alcohol</sub>.

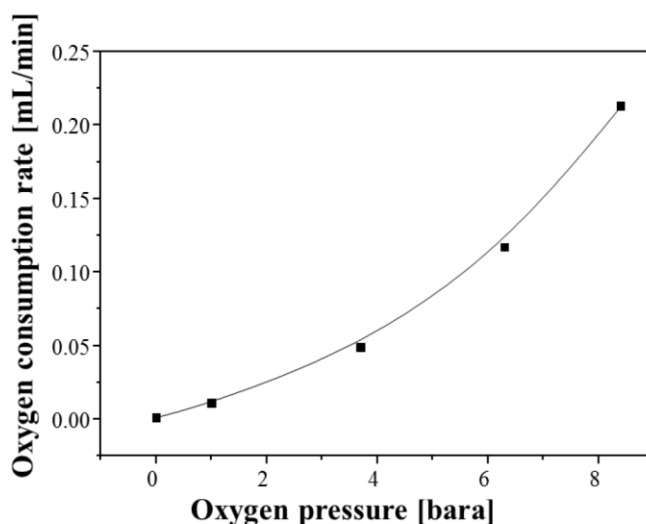


**Figure 5.** Oxygen consumption rates at STP under different oxygen pressures. Reaction conditions: Au-Pd/TiO<sub>2</sub> catalyst (90-125 μm), 100 mg; neat benzyl alcohol, 10 μL/min; catalyst contact time, 577 g<sub>cat</sub>·s/g<sub>alcohol</sub>; liquid pressure, 10 bara; reaction temperature, 120 °C.

The oxygen consumption rate at STP under different oxygen pressures is shown in Figure 5. Higher oxygen consumption rates were observed at higher gas pressure. The maximum rate was 0.21 mL/min (STP, 0.56 mmol/h) at 8.4 bara. The fact that the oxygen consumption rate was close to zero at 0 bara oxygen pressure (nitrogen was used in the gas channel), indicates that the amount of oxygen consumed in the reaction at elevated oxygen pressure comes from oxygen permeating through the membrane during the reaction. On the basis that all other reaction conditions were kept the same and only the oxygen pressure was changed,

increasing the oxygen pressure could therefore enhance the oxygen consumption and result in higher oxygen permeation.

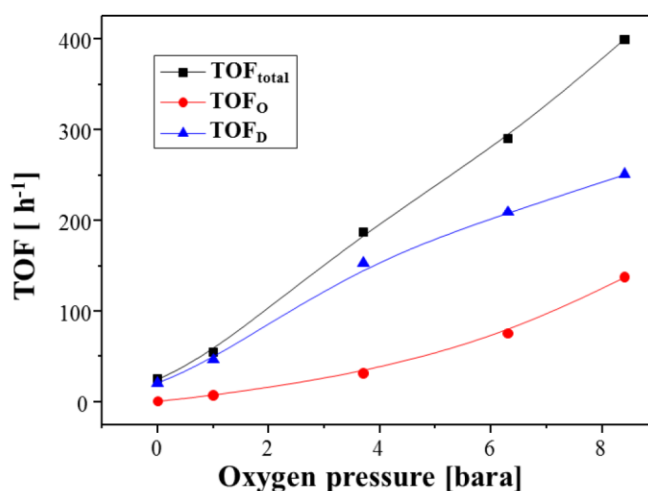


**Figure 6.** Average turnover frequencies under different oxygen pressures. Reaction conditions: Au-Pd/TiO<sub>2</sub> catalyst (90-125 μm), 100 mg; neat benzyl alcohol, 10 μL/min; catalyst contact time, 577 g<sub>cat</sub>·s/g<sub>alcohol</sub>; liquid pressure, 10 bara; reaction temperature, 120 °C.

To further investigate the effect of oxygen pressure on the reaction, TOFs under different oxygen pressures are calculated and shown in Figure 6. In the absence of oxygen (0 bara oxygen pressure), TOF<sub>total</sub> was very close to TOF<sub>D</sub>, and TOF<sub>O</sub> was practically zero. This indicates that disproportionation was the only reaction occurring and no oxidation reaction was taking place under these conditions [28]. With a rise in oxygen pressure, both TOF<sub>D</sub> and TOF<sub>O</sub> presented an upward trend without reaching a plateau. This contributed to an approximately linear increase in TOF<sub>total</sub>, as well as the increasing selectivity to benzaldehyde as shown in Figure 4. Since oxygen solubility in the liquid is increased at elevated oxygen pressure, this demonstrates that oxygen could promote both disproportionation and oxidation reactions [32], and thus have a positive effect on the oxidation of benzyl alcohol in the flat membrane reactor with Au-Pd/TiO<sub>2</sub> catalyst. Higher TOF<sub>total</sub> and TOF<sub>O</sub> were observed in batch reactors and trickle bed reactors, when higher oxygen pressure was used [33]. However, TOF<sub>D</sub> in both batch and trickle bed reactors was observed to decrease with oxygen pressure

higher than 1 bara [33, 34], This can be due to the twofold effect of oxygen on the disproportionation reaction possibly caused by the two different mechanisms for the disproportionation reaction, one anaerobic and the other anaerobic [27, 28]. At low oxygen pressure, the increase of oxygen pressure could promote the disproportionation reaction, but the promotion effect was reduced with further increasing oxygen pressure. Moreover, TOFs obtained in the flat membrane reactor ( $\text{TOF}_{\text{total}}, 400 \text{ h}^{-1}$  at 8.4 bara) were about two orders of magnitude lower than those reported in batch reactors using 2.5 wt% Au-2.5 wt% Pd/TiO<sub>2</sub> catalyst ( $\text{TOF}_{\text{total}}, 26,400 \text{ h}^{-1}$ ) [26]. Since the  $\text{TOF}_{\text{D}}$  was not observed to decrease in the flat membrane reactor and much lower TOFs were obtained, the flat membrane microchannel reactor might not supply oxygen efficiently as the batch and trickle bed reactors. So, the oxygen transfer resistance in the flat membrane microchannel reactor was investigated in the following sections.

### 3.4 Effect of membrane thickness

The effect of membrane thickness was investigated through placing a single-layer (0.07 mm thickness) or a double-layer (0.14 mm thickness) membrane in the microchannel reactor. The results at different catalyst contact times are shown in Figure 7. The same trend was observed for the conversion and selectivities under different catalyst contact times, that is, increasing the catalyst contact time enhanced both the conversion of benzyl alcohol and the selectivity to benzaldehyde, while decreasing the selectivity to toluene. This trend agrees with our previous results in the membrane reactors [17, 23], but differs from those obtained in batch and trickle bed reactors [27, 28], in which the selectivities were similar under different catalyst contact times. This is probably caused by the low efficiency of oxygen supply in the membrane reactors as discussed in Section 3.3. Longer catalyst contact time in the membrane reactor could contribute to longer time for both oxygen permeation and reaction, and thus

more oxygen supply per liquid volume [23]. This could further promote the oxidation reaction, resulting in the increasing of the selectivity to benzaldehyde.

Notably, a conversion of benzyl alcohol of 70% with 71% selectivity to benzaldehyde was obtained at  $1150 \text{ g}_{\text{cat}} \cdot \text{s} / \text{g}_{\text{alcohol}}$  and 8.4 bara oxygen pressure with single-layer membrane. At the same reaction conditions with double-layer membrane, the conversion and benzaldehyde selectivity were observed to be both 68%. When comparing the oxygen consumption rates under different membrane thicknesses (shown in Figure 7c), higher rate was observed for single-layer membrane at each catalyst contact time. The average oxygen consumption rate with single-layer membrane (0.19 mL/min) was 27% higher than that with double-layer (0.15 mL/min). This reveals that oxygen transfer resistance exists in the membrane. However, the oxygen transfer resistance in the membrane seems not to be the main transfer resistance, since only 27% increase of average oxygen consumption rate was observed when halving the membrane thickness (*i.e.*, halving the oxygen transfer resistance in the membrane).

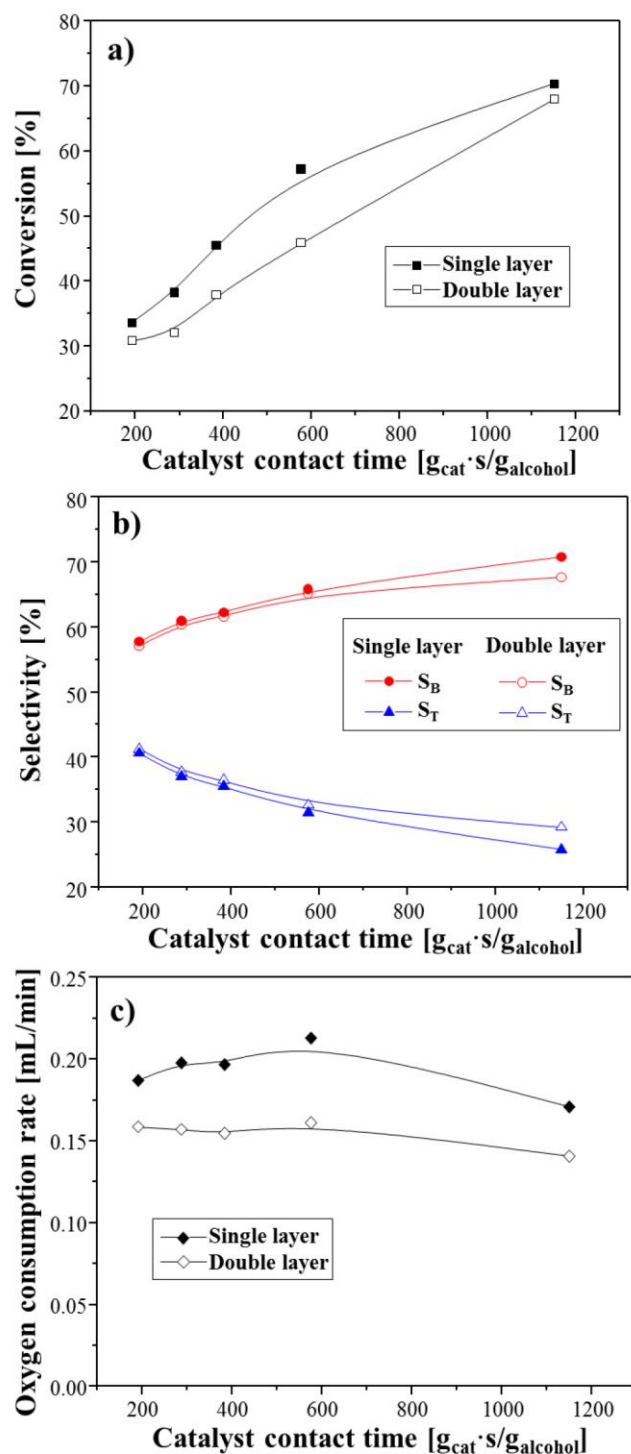


**Figure 7.** Effect of membrane thickness on the conversion, selectivities and oxygen consumption rate during oxidation of benzyl alcohol in the flat membrane microchannel reactor. Single layer, 0.07 mm; double layer, 0.14 mm. Reaction conditions: Au-Pd/TiO<sub>2</sub> catalyst (90-125  $\mu\text{m}$ ), 100 mg; neat benzyl alcohol, 5-30  $\mu\text{L}/\text{min}$ ; oxygen pressure: 8.4 bara; liquid pressure, 10 bara; reaction temperature, 120  $^{\circ}\text{C}$ .

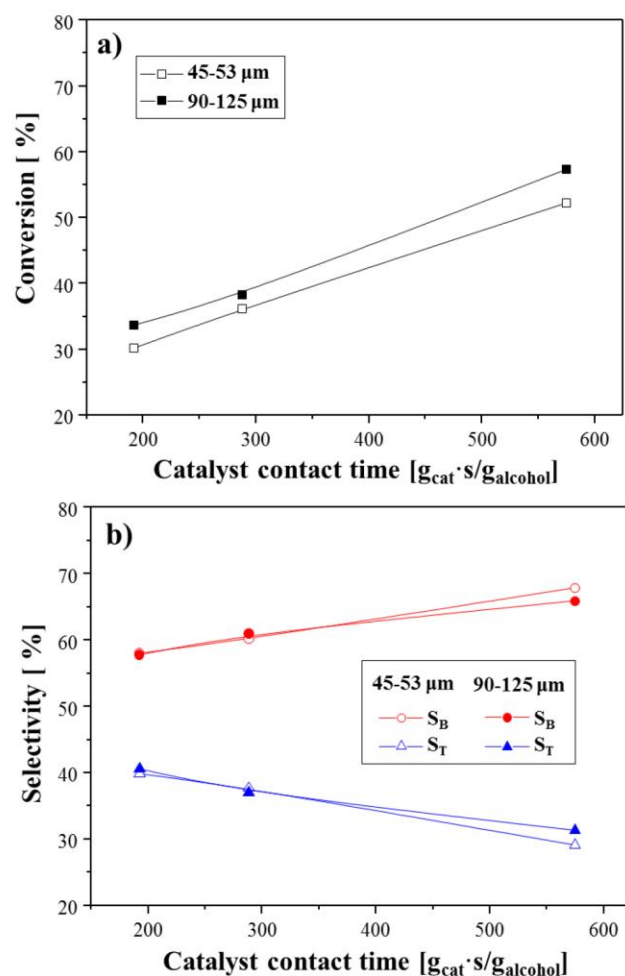


**Figure 8.** Effect of catalyst particle size on the conversion and selectivities during oxidation of benzyl alcohol in the flat membrane microchannel reactor. Reaction conditions: Au-Pd/TiO<sub>2</sub> catalyst, 100 mg; oxygen pressure: 8.4 bara; liquid pressure, 10 bara; reaction temperature, 120 °C.

**Table 1.** Comparison of TOFs for different liquid flow rates. Reaction conditions: Au-Pd/TiO<sub>2</sub> catalyst (90-125 μm), 50 or 100 mg; catalyst contact time, 192-577 g<sub>cat</sub>·s/g<sub>alcohol</sub>; oxygen pressure: 8.4 bara; liquid pressure, 10 bara; reaction temperature, 120 °C.

CCT [g <sub>cat</sub> ·s/g <sub>alcohol</sub> ]	577			288			192		
Catalyst weight [mg]	50	100	-	50	100	-	50	100	-
Liquid flow rate [uL/min]	5	10	$\frac{\text{TOF}_{10}}{\text{TOF}_5}$	10	20	$\frac{\text{TOF}_{20}}{\text{TOF}_{10}}$	15	30	$\frac{\text{TOF}_{30}}{\text{TOF}_{15}}$
TOF <sub>total</sub> [h <sup>-1</sup> ]	386	400	1.03	468	534	1.14	548	704	1.28
TOF <sub>O</sub> [h <sup>-1</sup> ]	143	138	0.96	139	128	0.92	137	121	0.88
TOF <sub>D</sub> [h <sup>-1</sup> ]	233	251	1.08	318	395	1.24	399	572	1.43

### 3.5 Internal/External mass transfer study

The internal mass transfer was studied using two ranges of catalyst particle sizes at different catalyst contact times. The conversion of benzyl alcohol and selectivities to benzaldehyde and toluene are shown in Figure 8a&b. Slightly higher conversion was observed when larger particles were used. This is possibly caused by the packed bed being slightly longer (caused by larger packed bed void volume) than that with small particles for the same catalyst weight, which contributes to longer time for oxygen permeation and reaction [23]. The selectivities to benzaldehyde and toluene were very similar, indicating independence on the catalyst particle size. Due to the unknown (and likely transversely and axially varying) oxygen concentration within the catalyst bed, the Weisz-Prater criterion cannot be used to quantitatively determine if internal diffusion is limiting the reaction. However, the results with the two catalyst particle sizes indicate that internal mass transfer resistance is not a determining factor for the performance of the system investigated.

The external mass transfer in the flat membrane microchannel reactor was studied through comparing the TOF under two different liquid flow rates at the same catalyst contact time. In Table 1, no clear difference was seen in all the TOFs when the liquid flow rate was increased from 5  $\mu\text{L}/\text{min}$  to 10  $\mu\text{L}/\text{min}$  at 577  $\text{g}_{\text{cat}}\cdot\text{s}/\text{g}_{\text{alcohol}}$ . When liquid flow rate was increased from 10  $\mu\text{L}/\text{min}$  to 20  $\mu\text{L}/\text{min}$  at shorter catalyst contact time (288  $\text{g}_{\text{cat}}\cdot\text{s}/\text{g}_{\text{alcohol}}$ ),  $\text{TOF}_{\text{total}}$  increased by 14%. This is caused by the increase of  $\text{TOF}_{\text{D}}$  (24%), despite the slight decrease in  $\text{TOF}_{\text{O}}$ . Higher increase of  $\text{TOF}_{\text{total}}$  (28%) was observed with liquid flow rate increasing from 15  $\mu\text{L}/\text{min}$  to 30  $\mu\text{L}/\text{min}$  at 192  $\text{g}_{\text{cat}}\cdot\text{s}/\text{g}_{\text{alcohol}}$ . A rise of 44% was also shown in  $\text{TOF}_{\text{D}}$ , together with 12% drop in  $\text{TOF}_{\text{O}}$ . The changes of  $\text{TOF}_{\text{O}}$  could be possibly caused by the experimental errors for the low conversions at high flow rate. However, the changes of  $\text{TOF}_{\text{D}}$  illustrate stronger influence of the liquid flow rate on the disproportionation reaction than the oxidation reaction.

The flat membrane microchannel reactor has been indicated to not supply oxygen efficiently as the batch and trickle bed reactors in Section 3.3 & 3.4. Note that the direction of oxygen transfer in the membrane reactor is perpendicular to that of liquid flow (in laminar flow regime), and oxygen needs to permeate the membrane, dissolve in the liquid, transversely transfer through the bulk liquid within the catalyst packed bed and reach the catalyst surface. Different liquid flow rates could potentially affect both the external mass transfer and the transverse mass transfer of oxygen in the bed, and thus affect the oxygen supply to the catalyst. The stronger influence of liquid flow rate on the disproportionation reaction can be possibly attributed to that the disproportionation reaction is more sensitive to oxygen at low oxygen supply due to the two different reaction mechanisms [27, 28]. A slight change of oxygen supply caused by the change of liquid flow rate may have a negligible effect on the oxidation reaction but a significant effect on the disproportionation reaction.

Based on the  $\text{TOF}_{\text{total}}$  ( $26,400 \text{ h}^{-1}$ ) and the selectivity to benzaldehyde ( $\sim 67\%$ ) obtained with 2.5 wt% Au-2.5 wt% Pd/TiO<sub>2</sub> catalyst in a batch reactor [26], the  $\text{TOF}_{\text{O}}$  of the Au-Pd/TiO<sub>2</sub> catalyst was calculated to be  $\sim 8800 \text{ h}^{-1}$  at 120 °C. This results to an oxygen demand of 13.6 mL/min at STP (36.5 mmol/h, calculation shown in the Supporting Information) for the amount of Au-Pd/TiO<sub>2</sub> catalyst packed in the membrane reactor (100 mg). The actual oxygen consumption rate within the membrane reactor was only 0.21 mL/min (0.56 mmol/h) at 8.4 bara oxygen pressure. This indicates a gap between oxygen demand by the highly active catalyst and oxygen supply in the membrane reactor. However, the maximum oxygen supply rate (the highest oxygen permeation rate) through the membrane area contacting the catalyst bed ( $\sim 50 \text{ mm} \times 3 \text{ mm}$ ) could be 0.93 mL/min (2.5 mmol/h) at 8.4 bara oxygen pressure, which is 4-fold of the oxygen consuming rate. The difference between the maximum oxygen supply rate and the actual oxygen consumption rate indicates oxygen transfer resistance in the catalyst bed. Since the internal/external mass transfer resistance

have been shown to have no significant effect on the oxidation reaction rate, the main oxygen transfer resistance is thus expected to exist in the bulk liquid within the catalyst bed.

### 3.6 Interaction of mass transfer processes with reaction in the packed bed membrane reactor

In order to assess the relative importance of the various mass transfer processes that affect reactor performance (membrane oxygen permeation and transverse mass transfer), an effectiveness factor ( $\eta$ ) is proposed based on the oxygen reaction rate (assumed as a first order in oxygen, the details are shown in the Supporting Information). By considering an analogy between our reactor and a single pellet where diffusion/reaction occurs, where the oxygen mass transfer through the membrane and transverse mass transfer in the reactor bed are analogous to external and internal mass transfer in a pellet respectively, we can use the standard effectiveness factor analysis.

To relate the reaction rate to the transverse mass transfer rate in the packed bed, a Damköhler number ( $Da$ ) is defined by

$$Da = \frac{d_1^2 k_{O_2}}{D_{O_2,T}} \quad (10)$$

where  $d_1$  is the depth of the packed bed (liquid channel),  $k_{O_2}$  is the oxygen reaction rate coefficient based on the bed volume,  $D_{O_2,T}$  is the transverse mass transfer coefficient of oxygen in the packed bed.

To provide a measure of oxygen permeation rate to oxygen transverse mass transfer rate, a Biot number ( $Bi$ ) is defined by

$$Bi = \frac{d_1 k_m}{D_{O_2,T}} \quad (11)$$

where  $k_m$  is the oxygen mass transfer coefficient in the Teflon AF-2400 membrane, and is inversely proportional to the membrane thickness (shown in the Supporting Information) [25].

So, akin to an overall effectiveness factor in terms of internal and external mass transfer in a single pellet [35], a *permeation-transverse mass transfer effectiveness factor* ( $\eta$ ) is described by

$$\eta = \frac{\sinh\sqrt{Da}}{\sqrt{Da}(\cosh\sqrt{Da} + \frac{\sqrt{Da}}{Bi} \sinh\sqrt{Da})} \quad (12)$$

For the Au-Pd/TiO<sub>2</sub> catalyst in the current flat membrane microchannel reactor, the Biot number is 85.2 (see the Supporting Information), which indicates that the oxygen permeation rate in the membrane is much higher than the oxygen transverse mass transfer rate in the packed bed. This results to slight increase of oxygen consumption rate when halving the membrane thickness. Using an estimated first-order reaction rate coefficient from the batch reactor, the Damköhler number is 5179, which suggests that the oxygen reaction in the membrane reactor is highly transverse mass transfer-controlled. The permeation-transverse mass transfer effectiveness factor is found to be 0.8%, which agrees well with the ratio (1.5%) of the observed TOFo in the membrane reactor ( $\sim 130 \text{ h}^{-1}$ ) to the batch reactor ( $\sim 8800 \text{ h}^{-1}$ ).

Since the oxygen transverse mass transfer rate is inversely proportional to the liquid channel depth, reduction in the liquid channel depth is expected to improve the performance of the membrane microchannel reactor for oxidation of benzyl alcohol. To confirm this, another flat membrane microchannel reactor was fabricated with half of liquid channel depth (0.5 mm) but the same channel width (3 mm) as compared to the previous design. The amount of packed catalyst was also halved to keep the length of catalyst bed the same. At the same catalyst contact time ( $577 \text{ g}_{\text{cat}} \cdot \text{s} / \text{g}_{\text{alcohol}}$ ) and oxygen pressure (8.4 bara), a 75% conversion of benzyl alcohol with a 67% selectivity to benzaldehyde was obtained in the 0.5 mm channel depth reactor, as compared to 57% conversion and 66% benzaldehyde selectivity

in the 1.0 mm channel depth reactor. This demonstrates that the main oxygen transfer resistance exists in the bulk liquid within the catalyst bed.

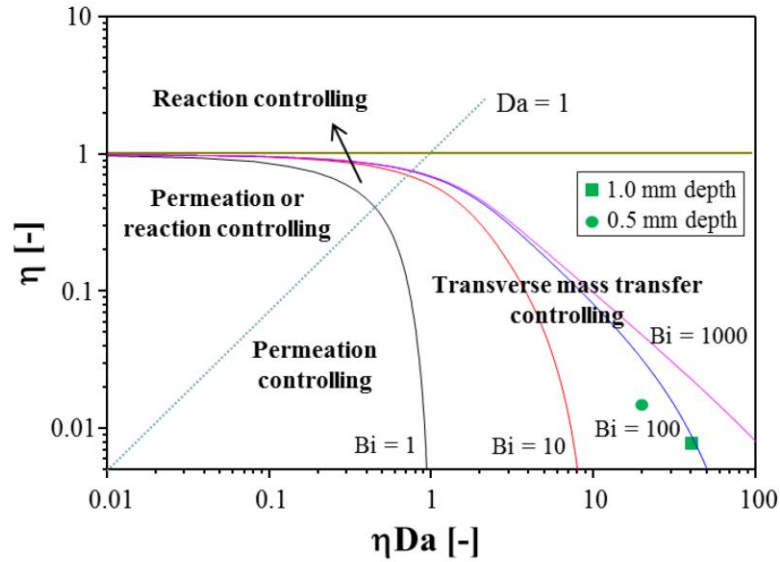


**Figure 9.** Permeation-transverse mass transfer catalytic effectiveness factor ( $\eta$ ) as a function of the observable  $\eta Da$  for various values of Biot number ( $Bi$ ) with the various regimes of possible controlling processes. (Symbols indicate the values for the current flat membrane reactor with liquid flow channel depth of 1.0 mm (■) and 0.5 mm (●))

To predict catalyst performance in the packed bed membrane reactor and guide reactor design, the effectiveness factor is shown as a function of an observable  $\eta Da$  for various values of Biot number analogous to Ref. [35] in Figure 9, together with the various regimes of possible controlling processes. When the reactor is in the transverse mass transfer controlling regime (as the symbols shown in Figure 9, which indicated the values for the flat membrane microchannel reactor with the liquid flow channel depth of 1.0 mm (■) and 0.5 mm (●), respectively), decreasing the channel depth can decrease the values of  $Da$  and  $Bi$ , which makes the effectiveness factor move towards the permeation or reaction controlling regime. When the reactor is in the permeation controlling regime, decreasing the membrane

thickness can increase the value of  $Bi$ , which makes the effectiveness factor move towards the reaction or transverse mass transfer controlling regime. Similarly, in the reaction controlling regime, the value of  $Da$  will increase if the reaction rate coefficient increased. This will make the effectiveness factor move towards the permeation or transverse mass transfer controlling regime.

### 3.7 Performance of the scaled-up membrane reactor

Scale-up of the flat membrane microchannel reactor was carried out through widening the channel width by  $\sim 10$  times, and the results are shown in Table 2. The reactor was kept vertical and the liquid flowed from top to bottom. As compared to the previous microchannel reactor (channel width, 3 mm), the scaled-up reactor presented a lower conversion of benzyl alcohol with a similar selectivity to benzaldehyde for the same catalyst contact time. The relative drop in conversion of  $\sim 17\%$  may be due to some fluid maldistribution in the wider liquid channel. Nevertheless, the benzaldehyde throughput was demonstrated to be increased by a factor of 8 in the scaled-up microchannel reactor.

**Table 2.** Comparison of reaction results in reactors with different channel width. Reaction conditions: Au-Pd/TiO<sub>2</sub> catalyst (90-125  $\mu\text{m}$ ); catalyst contact time, 1150  $\text{g}_{\text{cat}} \cdot \text{s} / \text{g}_{\text{alcohol}}$ ; liquid pressure, 10 bara; reaction temperature, 120 °C.

Reactor	Channel width [mm]	Catalyst packed [g]	Liquid flow rate [ $\mu\text{L}/\text{min}$ ]	Oxygen pressure [bar]	X [%]	S <sub>B</sub> [%]	S <sub>T</sub> [%]
Small	3	0.1	5	8.4	70	71	26
Large	32	1.0	50	8.2	58	69	26

**Table 3.** Effect of liquid flow direction on the performance of scaled-up microchannel reactor. Reaction conditions: Au-Pd/TiO<sub>2</sub> catalyst (90-125  $\mu\text{m}$ ), 1.0 g; liquid flow rate, 50  $\mu\text{L}/\text{min}$ ; catalyst contact time, 1150  $\text{g}_{\text{cat}} \cdot \text{s} / \text{g}_{\text{alcohol}}$ ; oxygen pressure, 8.2 bara; liquid pressure, 10 bara; reaction temperature, 120 °C.

Flow directions	a)	b)	c)
			
X [%]	58	55	54
S <sub>B</sub> [%]	69	66	67
S <sub>T</sub> [%]	26	30	29

The effect of liquid flow direction on the performance of the scaled-up microchannel reactor was further investigated with the same catalyst packing. The reactor was kept vertical with liquid flowing from top to bottom (Table 3a), reverse (Table 3b), or horizontal with liquid flowing from left to right (Table 3c). As shown in Table 3a, the conversion of benzyl alcohol was slightly lower (~5%) under the same conditions to that in Table 2, which could be caused by a slight catalyst deactivation after ~50 h reaction. However, for the three different flow directions, no obvious difference was observed in terms of conversion and selectivities. This indicates that the liquid flow direction has no effect on the liquid distribution within the liquid channel.

Finally, oxidation of benzyl alcohol was carried out with air in the scaled-up flat membrane microchannel reactor, since air is cheaper and easier use as compared to pure oxygen. As shown in Figure S8, the conversion of benzyl alcohol was 27%, with a selectivity of 63% to benzaldehyde. Under the same reaction conditions with pure oxygen, the conversion and selectivity to benzaldehyde were 65% and 68%, respectively. The different performance in terms of conversion and selectivity was caused by the different partial pressures of oxygen; as discussed in Figure 4, oxygen is beneficial for both conversion and benzaldehyde selectivity. These results highlight the efficiency of using pure oxygen, suggesting that to achieve similar performance with air, higher gas pressure would need to be utilised.

#### **4. Conclusions**

A Teflon AF-2400 flat membrane microchannel reactor was developed and applied for continuous-flow aerobic oxidation of solvent-free benzyl alcohol on Au-Pd/TiO<sub>2</sub> catalyst. As compared to a previous tube-in-tube membrane microreactor, the flat configuration provides

wider operating pressure range and is easier to scale up. The reactor can be combined with plate heat exchangers to realize better temperature control for highly exothermic reactions. Higher reaction rates and main product selectivities were observed at higher oxygen pressure, highlighting the importance of oxygen concentration for this reaction. Study of the various oxygen transfer processes (permeation through membrane, transverse mass transfer in the catalyst bed, internal/external transfer in the catalyst particles) indicated that the main oxygen transfer resistance was in the catalyst bed. This agreed with an effectiveness factor analysis akin to internal/external mass transfer and reaction in a catalytic particle, which further provides guidance on catalyst choice and membrane reactor design. Scale-up of the microchannel reactor by an order of magnitude was demonstrated by increasing the width of the catalyst bed channel. The simple assembly of the flat membrane microchannel reactor suggests that other similar flat membranes could be used for scalable flow oxidation of alcohols with molecular oxygen.

### **Acknowledgements**

The assistance of Ian Briggs (Johnson Matthey) with ICP analysis is appreciated. Financial support by EPSRC, UK (grant EP/L003279/1) is gratefully acknowledged.

### **References**

- [1] T. Mallat, A. Baiker, Oxidation of Alcohols with Molecular Oxygen on Solid Catalysts, *Chem. Rev.*, 104 (2004) 3037-3058.
- [2] C. Della Pina, E. Falletta, L. Prati, M. Rossi, Selective Oxidation Using Gold, *Chem. Soc. Rev.*, 37 (2008) 2077-2095.
- [3] S. Caron, R.W. Dugger, S.G. Ruggeri, J.A. Ragan, D.H.B. Ripin, Large-Scale Oxidations in the Pharmaceutical Industry, *Chem. Rev.*, 106 (2006) 2943-2989.
- [4] R. Ciriminna, V. Pandarus, F. Béland, Y.-J. Xu, M. Pagliaro, Heterogeneously Catalyzed Alcohol Oxidation for the Fine Chemical Industry, *Org. Process Res. Dev.*, 19 (2015) 1554-1558.
- [5] H.P.L. Gemoets, Y. Su, M. Shang, V. Hessel, R. Luque, T. Noel, Liquid Phase Oxidation Chemistry in Continuous-Flow Microreactors, *Chem. Soc. Rev.*, 45 (2016) 83-117.

- [6] Z. Guo, B. Liu, Q. Zhang, W. Deng, Y. Wang, Y. Yang, Recent Advances in Heterogeneous Selective Oxidation Catalysis for Sustainable Chemistry, *Chem. Soc. Rev.*, 43 (2014) 3480-3524.
- [7] M. Sankar, N. Dimitratos, P.J. Miedziak, P.P. Wells, C.J. Kiely, G.J. Hutchings, Designing Bimetallic Catalysts for a Green and Sustainable Future, *Chem. Soc. Rev.*, 41 (2012) 8099-8139.
- [8] S.E. Davis, M.S. Ide, R.J. Davis, Selective Oxidation of Alcohols and Aldehydes over Supported Metal Nanoparticles, *Green Chem.*, 15 (2013) 17-45.
- [9] D.S. Mannel, S.S. Stahl, T.W. Root, Continuous Flow Aerobic Alcohol Oxidation Reactions Using a Heterogeneous Ru(OH)<sub>x</sub>/Al<sub>2</sub>O<sub>3</sub> Catalyst, *Org. Process Res. Dev.*, 18 (2014) 1503-1508.
- [10] A. Gavriilidis, A. Constantinou, K. Hellgardt, K.K. Hii, G.J. Hutchings, G.L. Brett, S. Kuhn, S.P. Marsden, Aerobic Oxidations in Flow: Opportunities for the Fine Chemicals and Pharmaceuticals Industries, *React. Chem. Eng.*, 1 (2016) 595-612.
- [11] X. Ye, M.D. Johnson, T. Diao, M.H. Yates, S.S. Stahl, Development of Safe and Scalable Continuous-Flow Methods for Palladium-Catalyzed Aerobic Oxidation reactions, *Green Chem.*, 12 (2010) 1180-1186.
- [12] J.F. Greene, J.M. Hoover, D.S. Mannel, T.W. Root, S.S. Stahl, Continuous-Flow Aerobic Oxidation of Primary Alcohols with a Copper(I)/TEMPO Catalyst, *Org. Process Res. Dev.*, 17 (2013) 1247-1251.
- [13] N. Zotova, K. Hellgardt, G.H. Kelsall, A.S. Jessiman, K.K. Hii, Catalysis in Flow: the Practical and Selective Aerobic Oxidation of Alcohols to Aldehydes and Ketones, *Green Chem.*, 12 (2010) 2157-2163.
- [14] A. Comite, A. Bottino, G. Capannelli, C. Costa, R. Di Felice, 4 - Multi-Phase Catalytic Membrane Reactors A2 - Basile, Angelo, in: *Handbook of Membrane Reactors*, Woodhead Publishing, 2013, pp. 152-187.
- [15] X. Tan, K. Li, Membrane Microreactors for Catalytic Reactions, *J. Chem. Technol. Biotechnol.*, 88 (2013) 1771-1779.
- [16] T. Noël, V. Hessel, Membrane Microreactors: Gas-Liquid Reactions Made Easy, *ChemSusChem*, 6 (2013) 405-407.
- [17] A. Constantinou, G. Wu, A. Corredera, P. Ellis, D. Bethell, G.J. Hutchings, S. Kuhn, A. Gavriilidis, Continuous Heterogeneously Catalyzed Oxidation of Benzyl Alcohol in a Ceramic Membrane Packed-Bed Reactor, *Org. Process Res. Dev.*, 19 (2015) 1973-1979.
- [18] H. Zhang, S.G. Weber, Teflon AF Materials, in: I.T. Horvath (Ed.) *Fluorous Chemistry*, Springer-Verlag Berlin, Berlin, 2012, pp. 307-337.
- [19] T.P. Petersen, A. Polyzos, M. O'Brien, T. Ulven, I.R. Baxendale, S.V. Ley, The Oxygen-Mediated Synthesis of 1,3-Butadiynes in Continuous Flow: Using Teflon AF-2400 to Effect Gas/Liquid Contact, *ChemSusChem*, 5 (2012) 274-277.
- [20] M. Brzozowski, M. O'Brien, S.V. Ley, A. Polyzos, Flow Chemistry: Intelligent Processing of Gas-Liquid Transformations Using a Tube-in-Tube Reactor, *Acc. Chem. Res.*, 48 (2015) 349-362.
- [21] C.A. Hone, D.M. Roberge, C.O. Kappe, The Use of Molecular Oxygen in Pharmaceutical Manufacturing: Is Flow the Way to Go?, *ChemSusChem*, 10 (2017) 32-41.
- [22] S.R. Chaudhuri, J. Hartwig, L. Kupracz, T. Kodanek, J. Wegner, A. Kirschning, Oxidations of Allylic and Benzylic Alcohols under Inductively-Heated Flow Conditions with Gold-Doped Superparamagnetic Nanostructured Particles as Catalyst and Oxygen as Oxidant, *Adv. Synth. Catal.*, 356 (2014) 3530-3538.
- [23] G. Wu, A. Constantinou, E. Cao, S. Kuhn, M. Morad, M. Sankar, D. Bethell, G.J. Hutchings, A. Gavriilidis, Continuous Heterogeneously Catalyzed Oxidation of Benzyl Alcohol Using a Tube-in-Tube Membrane Microreactor, *Ind. Eng. Chem. Res.*, 54 (2015) 4183-4189.

- [24] J.F. Greene, Y. Preger, S.S. Stahl, T.W. Root, PTFE-Membrane Flow Reactor for Aerobic Oxidation Reactions and Its Application to Alcohol Oxidation, *Org. Process Res. Dev.*, 19 (2015) 858-864.
- [25] L. Yang, K.F. Jensen, Mass Transport and Reactions in the Tube-in-Tube Reactor, *Org. Process Res. Dev.*, 17 (2013) 927-933.
- [26] D.I. Enache, J.K. Edwards, P. Landon, B. Solsona-Espriu, A.F. Carley, A.A. Herzing, M. Watanabe, C.J. Kiely, D.W. Knight, G.J. Hutchings, Solvent-Free Oxidation of Primary Alcohols to Aldehydes Using Au-Pd/TiO<sub>2</sub> Catalysts, *Science*, 311 (2006) 362-365.
- [27] E. Cao, M. Sankar, S. Firth, K.F. Lam, D. Bethell, D.K. Knight, G.J. Hutchings, P.F. McMillan, A. Gavriilidis, Reaction and Raman Spectroscopic Studies of Alcohol Oxidation on Gold-Palladium Catalysts in Microstructured Reactors, *Chem. Eng. J.*, 167 (2011) 734-743.
- [28] M. Sankar, E. Nowicka, R. Tiruvalam, Q. He, S.H. Taylor, C.J. Kiely, D. Bethell, D.W. Knight, G.J. Hutchings, Controlling the Duality of the Mechanism in Liquid-Phase Oxidation of Benzyl Alcohol Catalysed by Supported Au-Pd Nanoparticles, *Chem.-Eur. J.*, 17 (2011) 6524-6532.
- [29] F. Galvanin, M. Sankar, S. Cattaneo, D. Bethell, V. Dua, G.J. Hutchings, A. Gavriilidis, On the Development of Kinetic Models for Solvent-Free Benzyl Alcohol Oxidation over a Gold-Palladium Catalyst, *Chem. Eng. J.*, 342 (2018) 196-210.
- [30] G. Wu, G.L. Brett, E. Cao, A. Constantinou, P. Ellis, S. Kuhn, G.J. Hutchings, D. Bethell, A. Gavriilidis, Oxidation of Cinnamyl Alcohol using Bimetallic Au-Pd/TiO<sub>2</sub> Catalysts: a Deactivation Study in a Continuous Flow Packed Bed Microreactor, *Catal. Sci. Tech.*, 6 (2016) 4749-4758.
- [31] M. Goethals, B. Vanderstraeten, J. Berghmans, G. De Smedt, S. Vliegen, E. Van't Oost, Experimental Study of the Flammability Limits of Toluene-Air Mixtures at Elevated Pressure and Temperature, *J Hazard Mater*, 70 (1999) 93-104.
- [32] M. Morad, M. Sankar, E. Cao, E. Nowicka, T.E. Davies, P.J. Miedziak, D.J. Morgan, D.W. Knight, D. Bethell, A. Gavriilidis, G.J. Hutchings, Solvent-Free Aerobic Oxidation of Alcohols Using Supported Gold Palladium Nanoalloys Prepared by a Modified Impregnation Method, *Catal. Sci. Tech.*, 4 (2014) 3120-3128.
- [33] E. Cao, M. Sankar, E. Nowicka, Q. He, M. Morad, P.J. Miedziak, S.H. Taylor, D.W. Knight, D. Bethell, C.J. Kiely, A. Gavriilidis, G.J. Hutchings, Selective Suppression of Disproportionation Reaction in Solvent-Less Benzyl Alcohol Oxidation Catalysed by Supported Au-Pd Nanoparticles, *Catal. Today*, 203 (2013) 146-152.
- [34] S. Meenakshisundaram, E. Nowicka, P.J. Miedziak, G.L. Brett, R.L. Jenkins, N. Dimitratos, S.H. Taylor, D.W. Knight, D. Bethell, G.J. Hutchings, Oxidation of alcohols using Supported Gold and Gold-Palladium Nanoparticles, *Faraday Discuss.*, 145 (2010) 341-356.
- [35] J.J. Carberry, *Chemical and Catalytic Reaction Engineering*, McGraw-Hill, New York, 1976.